2006

Novel Geometrical Model of Scroll Compressors for the Analytical Description of the Chamber Volumes

Benjamin Blunier
University of Technology of Belfort-Montbéliasd

Giansalvo Cirrincione
University of Picardie-Jules Verne

Abdellatif Miraoui
University of Technology of Belfort-Montbéliasd

NOVEL GEOMETRICAL MODEL OF SCROLL COMPRESSORS FOR THE ANALYTICAL DESCRIPTION OF THE CHAMBER VOLUMES

Benjamin BLUNIER[1,*], Giansalvo CIRRINCIONE[2], Abdellatif MIRAOUI[1]

[1]Laboratory in Electrical Engineering and Systems, L2ES
University of Technology of Belfort-Montbéliard, UTBM
UTBM (Bât. F) – 13, rue Thierry Mieg – 90010 Belfort, France
email: `benjamin.blunier@utbm.fr`

[2]Department of Electrical Engineering
University of Picardie-Jules Verne
33, rue Saint Leu – 80039 Amiens, France
email: `g.cirrincione@ieee.org`

[*]Corresponding author

ABSTRACT

Most scroll compressor models are based on a geometrical description of the scroll wraps. Since geometry is one of the main factors affecting the efficiency of the compressor, a complete description of the geometry of scroll wraps has to be known in order to establish an accurate thermodynamic model. Most authors do not yield an analytical expression of the discharge chamber, also because their assumptions are questionable. This paper gives a novel description of the geometry based on the parametric equations for the circle involutes in a novel reference system, in order to exploit the symmetry of the compressor. This approach simplifies the scroll model and yields an exact analytical expression of the compression and discharge chamber volumes, together with all the geometrical parameters and constraints, thus allowing the compressor to be optimized geometrically. The existence conditions of the conjugacy points, as well as the manufacturing constraints are also considered.

1. INTRODUCTION

The scroll compressor is a machine used for compressing air or refrigerant, which was originally invented in 1905 by a French engineer named Léon Creux (Creux, 1905). The device consists of two nested identical scrolls constituted in the classical design by involutes of circle as shown in FIG. 1(a). The two scrolls, whose axes of rotation do not meet each other, are assembled with a relative angle of π, so that they touch themselves at different points and form a series of growing size chambers.

The main advantages of the scroll compressor are the small number of moving parts, a high efficiency and a low level of noise and vibrations. However, one of the main problems encountered in developing scroll compressors is the design of the scroll profile which plays a key role in their performances.

Many geometric shapes for scroll compressors have been investigated in a lot of papers and patents. Most of the works have focused only on the interpolating curves by using circle involutes (Lee and Wu, 1995; Hirano et al., 1990; Chen et al., 2002; Halm, 1997). One of the authors (Gravensen et al., 1998; Gravensen and Henriksen, 2001) redefined the entire geometry of the spiral with two planar curves where the involute is a special case.

This paper proposes a new way to describe the geometry inspired by the work of Halm (1997) where the symmetries can be exploited and the optimization can be made taking into account the physical constraints.

2. FIXED SPIRAL GEOMETRY

2.1 Circle involutes

The shape of the investigated scroll can be described by an involute of circle. The scroll is therefore defined by two involutes that develop around a common basic circle with radius r_b and are offset by a constant distance. The fixed spiral can be described by:

$\forall\, \varphi \in \mathbf{I}_{fo} = [\varphi_{os},\, \varphi_{\text{max}}]$

$$\mathcal{S}_{fo} \left\{ \begin{array}{rcl} x_{fo}(\varphi) & = & r_b(\cos\varphi + \varphi\,\sin\varphi) \\ y_{fo}(\varphi) & = & r_b(\sin\varphi - \varphi\,\cos\varphi) \end{array} \right. \tag{1}$$

$\forall\, \varphi \in \mathbf{I}_{fi} = [\varphi_{is} - \varphi_{i0},\, \varphi_{\text{max}} - \varphi_{i0}]$

$$\mathcal{S}_{fi} \left\{ \begin{array}{rcl} x_{fi}(\varphi) & = & r_b(\cos(\varphi + \varphi_{i0}) + \varphi\,\sin(\varphi + \varphi_{i0})) \\ y_{fi}(\varphi) & = & r_b(\sin(\varphi + \varphi_{i0}) - \varphi\,\cos(\varphi + \varphi_{i0})) \end{array} \right. \tag{2}$$

where $\mathcal{S}_{fo}$ and $\mathcal{S}_{fi}$ are respectively the outer and inner involutes. The angles φ_{os} and φ_{is} are the outer and inner starting angles, φ_{max} the involute ending angle and φ_{i0} the initial angle of the inner involute.

The thickness of the scroll is

$$e = r_b\,\varphi_{i0} \quad \text{with } \varphi_{i0} > 0. \tag{3}$$

2.2 Interpolating circle

The involutes describing the scroll start at an outer angle φ_{os} at A_o ($\mathcal{S}_{fo}(\varphi_{os})$) and an inner angle φ_{is} at A_i ($\mathcal{S}_{fi}(\varphi_{is} - \varphi_{i0})$), respectively, and are connected by an arc belonging to the circle $\mathcal{C}_c$, constrained to be tangent to the inner involute at A_i as shown in FIG. 1(b). Hence the circle equations can be written as:

$$\mathcal{C}_c = \left\{ \begin{array}{rcl} x_{\mathcal{C}}(\varphi) & = & r_c(t_c)\,\cos(\varphi) + x_c(t_c) \\ y_{\mathcal{C}}(\varphi) & = & r_c(t_c)\,\sin(\varphi) + y_c(t_c) \end{array} \right. \tag{4}$$

where

$$\left\{ \begin{array}{rcl} x_c(t) & = & t \\ y_c(t) & = & a_m\,t + b_m \\ r_c(t) & = & \sqrt{\left(x_c(t) - x_{fi}(\varphi_{is} - \varphi_{i0})\right)^2 + \left(y_c(t) - y_{fi}(\varphi_{is} - \varphi_{i0})\right)^2} \\ t_c & = & \dfrac{x_{fi}(\varphi_{is} - \varphi_{i0}) + \left(y_{fi}(\varphi_{is} - \varphi_{i0}) - b_m\right)\,\tan(\varphi_{is})}{1 + a_m\,\tan(\varphi_{is})} \\ a_m & = & -\dfrac{x_{fi}(\varphi_{is} - \varphi_{i0}) - x_{fo}(\varphi_{os})}{y_{fi}(\varphi_{is} - \varphi_{i0}) - y_{fo}(\varphi_{os})} \\ b_m & = & \dfrac{\left(y_{fi}(\varphi_{is} - \varphi_{i0})^2 - y_{fo}(\varphi_{os})^2\right) + \left(x_{fi}(\varphi_{is} - \varphi_{i0})^2 - x_{fo}(\varphi_{os})^2\right)}{2\left(y_{fi}(\varphi_{is} - \varphi_{i0}) - y_{fo}(\varphi_{os})\right)} \end{array} \right.$$

Depending on φ_{is} and φ_{os}, the circle, as seen from the outside of the scroll, can be either concave (FIG. 2(a)) or convex (FIG. 2(b)). The concavity/convexity condition can be deduced from the relative positions of the vectors $\overrightarrow{\tau}$ and $\overrightarrow{OA_i}$,

$$\overrightarrow{\tau}(\varphi_{is} - \varphi_{i0}) \wedge \overrightarrow{OA_i} \left\{ \begin{array}{lll} < 0 & \text{concavity} & \rightarrow \text{ the circle goes from } A_i \text{ to } A_o \text{ (FIG. 2(a))} \\ > 0 & \text{convexity} & \rightarrow \text{ the circle goes from } A_o \text{ to } A_i \text{ (FIG. 2(b))} \end{array} \right. \tag{5}$$

Moreover,

$$\overrightarrow{\tau} \wedge \overrightarrow{OA_i} = r_b^2\,(\varphi_{is} - \varphi_{i0}) \frac{c_1\,\cos(\varphi_{os} - \varphi_{is}) - c_2\,\sin(\varphi_{os} - \varphi_{is}) + c_3}{\varphi_{os}\,\cos(\varphi_{os} - \varphi_{is}) - \sin(\varphi_{os} - \varphi_{is}) + (\varphi_{i0} - \varphi_{is})} \tag{6}$$

where

$$\left\{ \begin{array}{rcl} c_1 & = & 2\left(\varphi_{os}\left(\varphi_{i0} - \varphi_{is}\right) - 1\right) \\ c_2 & = & 2\left(\varphi_{os} + \varphi_{i0} - \varphi_{is}\right) \\ c_3 & = & \varphi_{os}^2 + \varphi_{i0}^2 - 2\,\varphi_{i0}\,\varphi_{is} + \varphi_{is}^2 + 2 \end{array} \right.$$

The existence domain $\mathbf{I}_\mathcal{C}$ of the circle is deduced from the previous conditions (5)

$$\mathbf{I}_\mathcal{C} = \begin{cases} [\varphi_i',\, \varphi_o'] & \text{if concave} \\ [\varphi_o',\, \varphi_i'] & \text{otherwise} \end{cases} \tag{7}$$

where

$$\varphi_i' = \begin{cases} \varphi_i - 2\pi & \text{if concave and } (\varphi_i > \varphi_o) \\ \varphi_i & \text{otherwise} \end{cases} \tag{8}$$

$$\varphi_o' = \begin{cases} \varphi_o - 2\pi & \text{if convex and } (\varphi_i < \varphi_o) \\ \varphi_o & \text{otherwise} \end{cases} \tag{9}$$

and

$$\varphi_i = \text{atan2}\Big(x_{fi}(\varphi_{is} - \varphi_{i0}) - x_c(t_c)\,,\, y_{fi}(\varphi_{is} - \varphi_{i0}) - y_c(t_c)\Big) \tag{10}$$

$$\varphi_o = \text{atan2}\Big(x_{fo}(\varphi_{os}) - x_c(t_c)\,,\, y_{fi}(\varphi_{os}) - y_c(t_c)\Big) \tag{11}$$

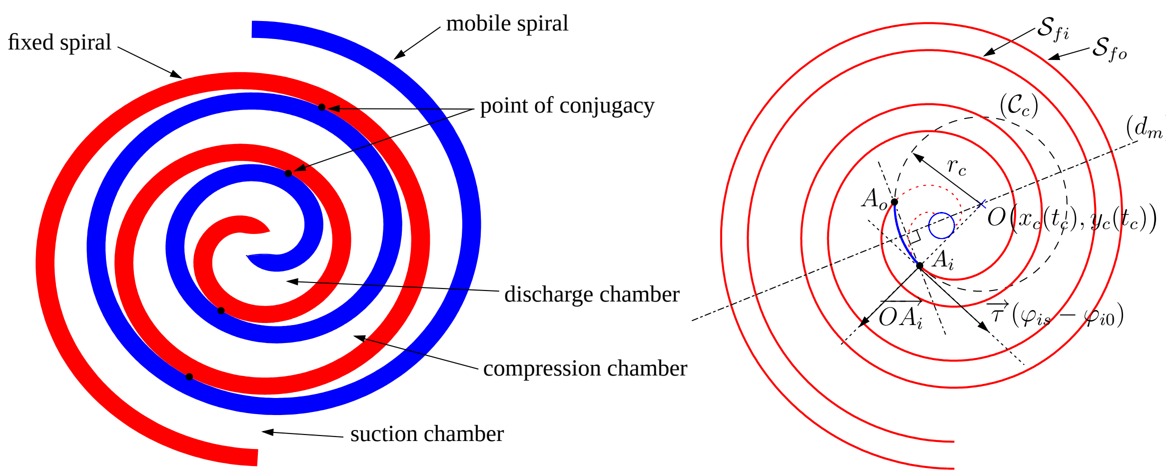

(a) Schematic view of a scroll compressor (b) Overview of a spiral

Figure 1: Schematic of a scroll compressor and the spiral

3. SCROLL COMPRESSOR GEOMETRY

3.1 Orbiting scroll

The geometry of the orbiting scroll is the same as the fixed one but is offset by π and the two scrolls are in conjugacy. Defining θ as the orbiting angle, it follows:

$\forall\, \varphi \in \mathbf{I}_{mo} = [\varphi_{os},\, \varphi_{\max}]$

$$\mathcal{S}_{mo} \begin{cases} x_{mo}(\varphi, \theta) = r_b(\cos(\varphi + \pi) + \varphi\, \sin(\varphi + \pi)) + r_o\, \cos(\theta + 3\pi/2) \\ y_{mo}(\varphi, \theta) = r_b(\sin(\varphi + \pi) - \varphi\, \cos(\varphi + \pi)) + r_o\, \sin(\theta + 3\pi/2) \end{cases} \tag{12}$$

$\forall\, \varphi \in \mathbf{I}_{mi} = [\varphi_{is} - \varphi_{i0},\, \varphi_{\max} - \varphi_{i0}]$

$$\mathcal{S}_{mi} \begin{cases} x_{mi}(\varphi, \theta) = r_b(\cos(\varphi + \varphi_{i0} + \pi) + \varphi\, \sin(\varphi + \varphi_{i0} + \pi)) + r_o\, \cos(\theta + 3\pi/2) \\ y_{mi}(\varphi, \theta) = r_b(\sin(\varphi + \varphi_{i0} + \pi) - \varphi\, \cos(\varphi + \varphi_{i0} + \pi)) + r_o\, \sin(\theta + 3\pi/2) \end{cases} \tag{13}$$

where r_o is the orbiting radius and $r_o = r_b\,(\pi - \varphi_{i0})$ with $0 < \varphi_{i0} < \pi$ and $r_b > 0$.

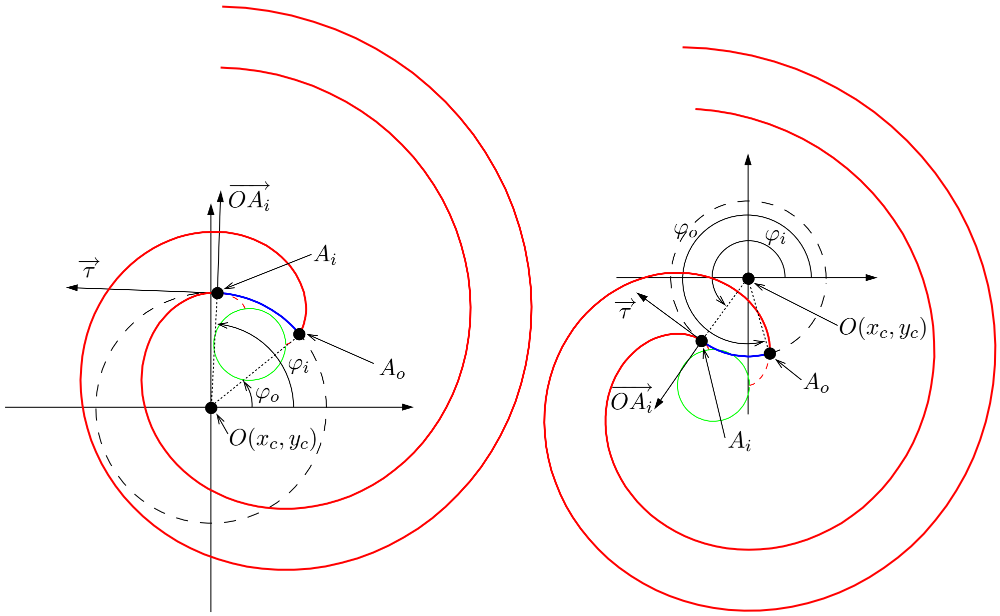

(a) Concavity

(b) Convexity

Figure 2: Convexity and concavity of the interpolating circle

3.2 Novel reference frame

In literature the reference frame shown in FIG. 3(a) is employed. Here a novel reference frame is presented (see FIG. 3(b)) in order to exploit the symmetry of the two scrolls. In this frame, the parametric equations of the fixed scroll are given by:

$$\mathcal{S}'_{fo} \left\{ \begin{array}{lcl} x'_{fo}(\varphi) & = & r_b(\cos\varphi + \varphi \, \sin\varphi) - 1/2\, r_o \, \cos(\theta + 3\,\pi/2) \\ y'_{fo}(\varphi) & = & r_b(\sin\varphi - \varphi \, \cos\varphi)) - 1/2\, r_o \, \cos(\theta + 3\,\pi/2) \end{array} \right. \tag{14}$$

$$\mathcal{S}'_{fi} \left\{ \begin{array}{lcl} x'_{fi}(\varphi) & = & r_b(\cos(\varphi + \varphi_{i0}) + \varphi \, \sin(\varphi + \varphi_{i0}))) - 1/2\, r_o \, \cos(\theta + 3\,\pi/2) \\ y'_{fi}(\varphi) & = & r_b(\sin(\varphi + \varphi_{i0}) - \varphi \, \cos(\varphi + \varphi_{i0}))) - 1/2\, r_o \, \cos(\theta + 3\,\pi/2) \end{array} \right. \tag{15}$$

and of the orbiting scroll are given by:

$$\mathcal{S}'_{mo} \left\{ \begin{array}{lcl} x'_{mo}(\varphi, \theta) & = & -x'_{fo}(\varphi, \theta) \\ y'_{mo}(\varphi, \theta) & = & -y'_{fo}(\varphi, \theta) \end{array} \right. \tag{16}$$

$$\mathcal{S}'_{mi} \left\{ \begin{array}{lcl} x'_{mi}(\varphi, \theta) & = & -x'_{fi}(\varphi, \theta) \\ y'_{mi}(\varphi, \theta) & = & -y'_{fi}(\varphi, \theta) \end{array} \right. \tag{17}$$

3.3 Points of conjugacy

The kth point of conjugacy $\varphi_{Cfimo-fi,k}$ between the fixed inner involute (fi) and the orbiting outer involute (mo) on the fixed inner involute (fi) is given by:

$$\varphi_{Cfimo-fi,k} = \theta - \varphi_{i0} + 2k\pi \quad k \in \mathbb{Z}. \tag{18}$$

The kth point of conjugacy $\varphi_{Cfimo-mo,k}$ between the fixed inner involute (fi) and the orbiting outer involute (mo) on the orbiting outer involute (mo) is given by:

$$\varphi_{Cfimo-mo,k} = \theta - \pi + 2k\pi \quad k \in \mathbb{Z}. \tag{19}$$

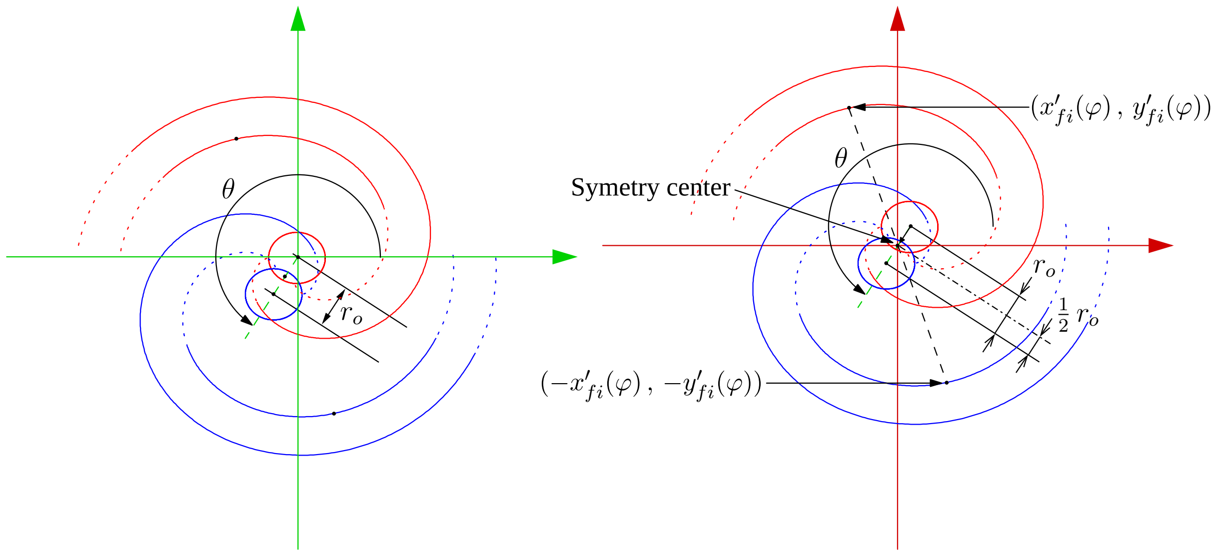

(a) Old reference frame (b) Novel reference frame

Figure 3: Novel reference frame

Using the same notations, the kth point of conjugacy between the fixed outer involute and the orbiting inner involute, repectively, on the fixed outer involute and the orbiting inner involute is given by:

$$\varphi_{Cfomi-fo,k} = \theta - \pi + 2k\pi \quad k \in \mathbb{Z}, \tag{20}$$

$$\varphi_{Cfomi-mi,k} = \theta - \varphi_{i0} + 2k\pi \quad k \in \mathbb{Z}. \tag{21}$$

Then, finally, the coordinates of the points of conjugacy are:

$$\text{fixed inner involute} \quad : \quad \left(x'_{fi}(\varphi_{Cfime-fi,k}\,,\,\theta)\,,\,y'_{fi}(\varphi_{Cfime-fi,k},\theta)\right) \tag{22}$$

$$\text{fixed outer involute} \quad : \quad \left(-x'_{fi}(\varphi_{Cfime-fi,k}\,,\,\theta)\,,\,-y'_{fi}(\varphi_{Cfime-fi,k},\theta)\right) \tag{23}$$

Assuming that for $k > 2$ being $k \in \{1..\alpha\}$, where α ($\alpha \in \mathbb{N}$) is the number of involute rotations (*i.e.*, $\varphi_{\max} = \alpha\, 2\pi$) all the points of conjugacy exist for all θ ($\theta \in]0,\, 2\pi]$), then it can be deduced:

$$\begin{cases} \varphi_{Cfimo-fi,k} = \theta - \varphi_{i0} + 2(k-1)\pi & k \in \{2..\alpha\},\ \forall\theta \in]0,\, 2\pi] \\ \varphi_{Cfimo-fi,1} = \theta - \varphi_{i0} & \text{exists if } \max(\varphi_{is}\,,\,\varphi_{os} + \pi) \leq \theta \end{cases} \tag{24}$$

where $0 \leq \varphi_{os} \leq \pi$ and $\varphi_{i0} \leq \varphi_{is} \leq 2\pi$.

4. ESTIMATION OF THE CHAMBER VOLUMES

4.1 Compression chamber

The surface of the kth compression chamber between the fixed inner involute and the orbiting outer involute can be computed straightforward by the involute between two consecutive points of conjugacy:

$$\begin{aligned} S_{fi,mo,k}(\theta) &= \frac{1}{2}\int_{\varphi_{Cfime-fi,k}}^{\varphi_{Cfime-fi,k+1}} \left(x'_{fi}\frac{\mathrm{d}y'_{fi}}{\mathrm{d}\varphi} - y'_{fi}\frac{\mathrm{d}x'_{fi}}{\mathrm{d}\varphi}\right)\mathrm{d}\varphi - \frac{1}{2}\int_{\varphi_{Cfime-me,k}}^{\varphi_{Cfime-me,k+1}} \left(x'_{mo}\frac{\mathrm{d}y'_{mo}}{\mathrm{d}\varphi} - y'_{mo}\frac{\mathrm{d}x'_{mo}}{\mathrm{d}\varphi}\right)\mathrm{d}\varphi \\ &= r_b^2\pi\,(\pi - \varphi_{i0})(4k\pi - 3\pi + 2\theta - \varphi_{i0}) \end{aligned} \tag{25}$$

Taking into account the existence conditions of the points of conjugacy:

$$\begin{cases} S_{fi,mo,k}(\theta) = r_b^2\pi\,(\pi - \varphi_{i0})(4k\pi - 3\pi + 2\theta - \varphi_{i0}) & \forall k \in [2..\alpha - 1] \\ S_{fi,mo,1}(\theta) = r_b^2\pi\,(\pi - \varphi_{i0})(4\pi - 3\pi + 2\theta - \varphi_{i0}) & \text{exists if } \max(\varphi_{is}, \varphi_{os} + \pi) \leq \theta \end{cases} \tag{26}$$

The volume is immediately deduced by multiplying it with the constant scroll height.

4.2 Discharge chamber

The computation of the surface of the discharge chamber takes into account the concavity and convexity cases (FIG. 4). The whole discharge surface S_d is computed in accordance with what is shown in FIG. 4:

$$S_d = \begin{cases} 2\,(S_1 + S_2) = 2\,(S_1 + S_{21} - S_{22} + S_{23}) & \text{if concave} \\ 2\,(S_1 + S_2) = 2\,(S_1 + S_{21} + S_{22} - S_{23}) & \text{otherwise} \end{cases} \tag{27}$$

where:

$$S_1 = \int_{\varphi_{is}-\varphi_{i0}}^{\varphi_{Cfomi-mi,k}} \left(x'_{mi}\frac{\mathrm{d}y'_{mi}}{\mathrm{d}\varphi} - y'_{mi}\frac{\mathrm{d}x'_{mi}}{\mathrm{d}\varphi} \right) \mathrm{d}\varphi - \int_{\varphi_{os}}^{\varphi_{Cfomi-fo,k}} \left(x'_{fo}\frac{\mathrm{d}y'_{fo}}{\mathrm{d}\varphi} - y'_{fo}\frac{\mathrm{d}x'_{fo}}{\mathrm{d}\varphi} \right) \mathrm{d}\varphi$$
$$\text{with } k = \begin{cases} 1 & \text{if } \max(\varphi_{is}, \varphi_{os} + \pi) \leq \theta \\ 2 & \text{otherwise} \end{cases} \tag{28}$$

$$S_{21} = A_t(0, 0, x_{A_i}, y_{A_i}, x_{A_o}, y_{A_o}) \tag{29}$$

$$S_{22} = \frac{1}{2} r_c(t_c)^2 |\varphi'_i - \varphi'_o| \tag{30}$$

$$S_{23} = A_t(x_c(t_c), y_c(t_c), x_{A_i}, y_{A_i}, x_{A_o}, y_{A_o}) \tag{31}$$

being $A_t(x_A, y_A, x_B, y_B, x_C, y_C)$ the area of triangle whose vertices are ABC, computed as:

$$A_t(x_A, y_A, x_B, y_B, x_C, y_C) = \frac{1}{2}|y_C \cdot x_A + x_C \cdot y_B - x_C \cdot y_A - y_C \cdot x_B + y_A \cdot x_B| \tag{32}$$

The volume is immediately deduced by multiplying it with the constant scroll height.
Two examples (concave and convex) are given in FIG. 5.

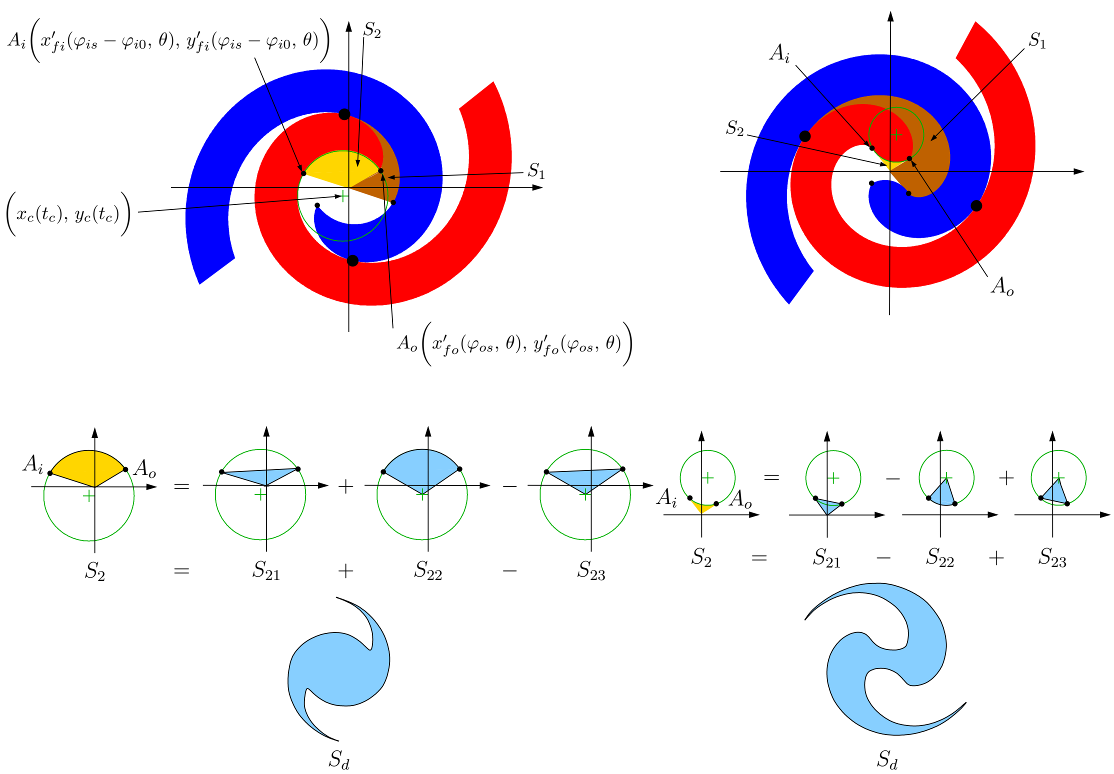

(a) Convex case (b) Concave case

Figure 4: Discharge chamber

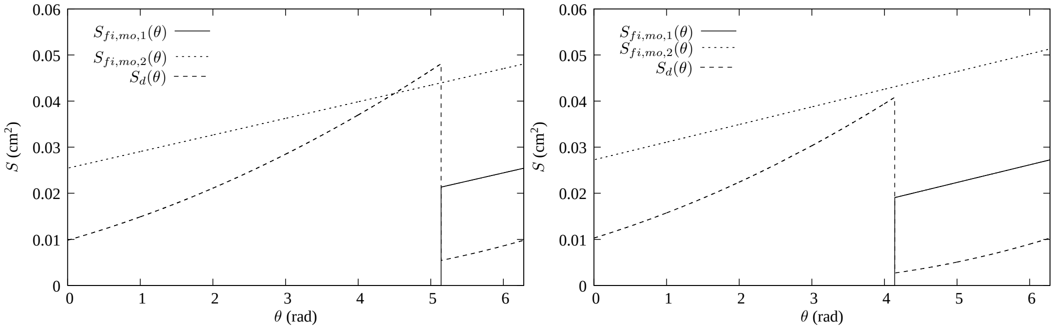

(a) Concave: $r_b = 1.91 \cdot 10^{-3}$ m, $\varphi_{is} = 2.571$ rad, $\varphi_{i0} = 1.571$ rad, $\varphi_{os} = 2$ rad

(b) Convex: $r_b = 1.91 \cdot 10^{-3}$ m, $\varphi_{is} = 3.471$ rad, $\varphi_{i0} = 1.471$ rad, $\varphi_{os} = 1$ rad

Figure 5: Surfaces of the chambers vs. orbiting angle (examples)

5. CONCLUSION

The efficiency of the scroll compressor is dictated by its geometry. Hence, a complete description of the model is required, also to determine an accurate thermodynamic model. For this purpose, a novel geometry description is proposed here. It exploits the symmetry of the scroll compressor by using a novel reference frame. This choice allows the scroll model to be simplified and yields exact analytical expressions for the compressor and discharge chamber volumes, together with all the geometrical parameters and constraints for the optimization of the scroll geometry.

REFERENCES

Chen, Y., Halm, N. P., Groll, E. A., Braun, J. E., 2002. Mathematical modeling of scroll compressor – part I: compression process modeling. International Journal of Refrigeration 25, 731–750.

Creux, L., 1905. Rotary engine. U.S Patent 801182.

Etemad, S., Nieter, J., 1989. Design optimization of the scroll compressor. International Journal of refrigeration 12, 146–150.

Gravensen, J., Henriksen, C., 2001. The geometry of the scroll compressor. Society for Industrial and Applied Mathematics 43 (1), 113–126.

Gravensen, J., Henriksen, C., Howell, P., 1998. Danfoss: Scroll optimization. Final report, Department of Mathematics, Technical University of Denmark, Lyngby, 32nd European Study Group with Industry.

Halm, N. P., 1997. Mathematical modeling of scroll compressor. Master's thesis, Herrick kab., School of Mechanical Engineering, Purdue University.

Hirano, T., Hagimoto, K., Maada, M., 1990. Scroll profiles for scroll fluid machines. MHI Tech Rev 27 (1), 35–41.

Lee, Y.-R., Wu, W.-F., 1995. On the profile design of a scroll compressor. International journal of refrigeration 18 (5), 308–317.

Morishita, E., Sugihara, M., Inaba, T., Nakamura, T., Works, W., 1984. Scroll compressor analytical model. In: Purdue International Compressor Engineering Conference Proceedings. pp. 487–495.

Tseng, C.-H., Chang, Y.-C., 2006. Family design of scroll compressors with optimization. Applied Thermal Engineering 26, 1074–1086.

ACKNOWLEDGEMENT

Giansalvo Cirrincione is with the Department of Electrical Engineering University of Picardie-Jules Verne and funded with a grant of ISSIA-CNR, Palermo, Italy in the framework of the project "Automazione della gestione intelligente della generazione distribuita di energia elettrica da fonti rinnovabili e non inquinanti e della domanda di energia elettrica, anche con riferimento alle compatibilità interne e ambientali, all'affidabilità e alla sicurezza".